Anal. Chem. **1995**, *67*, 2619–2624

Reverse Differential Pulse Voltammetry and Polarography

Luis Camacho* and Juan José Ruiz

Departamento de Química Física y Termodinámica Aplicada, Facultad de Ciencias, Universidad de Córdoba, c/San Alberto Magno s/n, E-14004 Córdoba, Spain

Carmen Serna,* Francisco Martínez-Ortiz, and Angela Molina

Departamento de Química Física, Facultad de Química, Universidad de Murcia, Campus de Espinardo, E-30100 Murcia, Spain

In this paper we obtain the analytical solution for the reverse differential pulse (RDP) technique for a slow electronic transfer process, starting from expressions obtained previously for the faradaic response to a triple potential pulse. The solutions are valid for the planar approximations of a static mercury drop electrode and of a dropping mercury electrode. An irreversible reduction process gives rise in the RDP technique to the appearance of two peaks, one at more negative potentials than the normal reduction potential, $E°$, and the other at more positive potentials than $E°$. From half-width peak and peak potential measurements, it is possible to evaluate approximately the kinetic and thermodynamic parameters corresponding to the electronic transfer, such as the transfer coefficient, α, the normal reduction potential, $E°$, and the apparent heterogeneous rate constant, k_s. The solutions are checked against experimental examples of well-known processes.

Among double-pulse electrochemical techniques, the reverse pulse (RP) technique is, undoubtedly, the most powerful from the kinetic point of view, due to the information that it provides on the degree of reversibility of electrode processes. This information is similar to that which can be obtained from cyclic voltammetry.[1] However, in spite of the fact that the theoretical treatment for a simple electrode process in the RP technique is mathematically solved,[2–5] experimental use of this technique has remained restricted, almost exclusively, to the analysis of the limiting currents of the signals obtained.[6–8] One reason for this could that when a quasi-reversible electronic transfer is analyzed using this technique, two very close waves are obtained, and these are difficult to resolve from an experimental viewpoint.

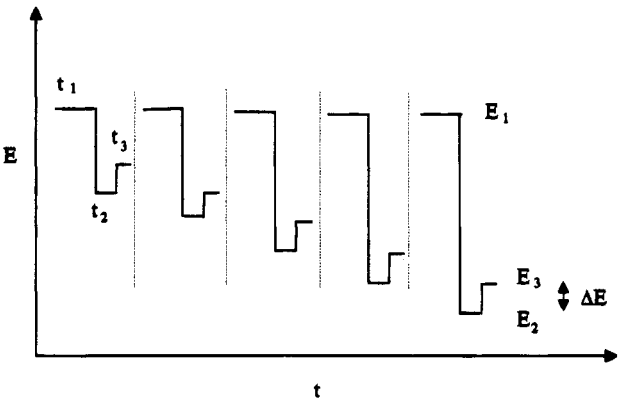

Figure 1. Potential–time wave form corresponding to the RDNP technique.

The above problem can be eliminated by using the reverse differential normal pulse (RDNP) technique. This technique was proposed by Brumleve et al.[9] and is based on the application of three potential pulses in accordance with the sequence described in Figure 1.

Potentials E_1 and E_2 are chosen as in the RP technique, i.e., E_1 is always constant and corresponds to a potential at which the reduction process is controlled by diffusion, whereas E_2 shifts to positive potentials. In the RDNP technique, we choose a potential E_3 such that $\Delta E = E_3 - E_2$ is constant. i_1, i_2, and i_3 are designated as the faradaic responses corresponding to each of the potentials, E_1, E_2, and E_3, which are applied during times t_1, t_2, and t_3, respectively.

RDNP is the name given to the technique based on the representation of $\Delta i = i_3 - i_2$ vs E_2.[9] The records obtained with this technique are peak-shaped, in opposition to the waves obtained in RP, with the corresponding analytical advantages that this implies. In this sense, the advantages of RDNP with respect to RP are similar to those which at the time brought about the introduction of the differential pulse polarography (DPP) technique with respect to classic polarography.

In a previous paper,[10] we studied the faradaic response of a slow electronic transfer to a triple potential pulse by applying the planar approximation to the static mercury drop electrode (SMDE)

(1) Osteryoung, J.; Murphy, M. In *Microelectrodes: Theory and Applications*. Montenegro, M. I., et al., Eds.; Kluwer Academic: the Netherlands, 1991, pp 123–138.
(2) Matsuda, H. *Bull. Chem. Soc. Jpn.* **1980**, *53*, 3439.
(3) Lovric, M.; Osteryoung, J. *Electrochim. Acta* **1982**, *27*, 963.
(4) Aoki, K.; Osteryoung, J.; Osteryoung, R. A. *J. Electroanal. Chem.* **1980**, *110*, 1.
(5) Aoki, K.; Osteryoung, J. *J. Electroanal. Chem.* **1980**, *110*, 19.
(6) Osteryoung, J.; Kirowa-Eisner, E. *Anal. Chem.* **1980**, *52*, 62.
(7) Brumleve, T. R.; Osteryoung, J. *J. Phys. Chem.* **1982**, *86*, 1794.
(8) Sinru, L.; Osteryoung, J.; O'Dea, J.; Osteryoung, R. A. *Anal. Chem.* **1988**, *60*, 1135.
(9) Brumleve, T. R.; Osteryoung, R. A.; Osteryoung, J. *Anal. Chem.* **1982**, *54*, 782.
(10) Serna, C.; Molina, A.; Camacho, L.; Ruiz, J. *J. Anal. Chem.* **1993**, *65*, 215.

0003-2700/95/0367-2619$9.00/0

and to the dropping mercury electrode (DME). The theoretical treatment is also valid for a solid electrode, provided that the boundary conditions are renewed, either by stirring or by employing a sufficiently long delay time at an initial potential at zero faradaic current.

In the present paper, we obtain the analytical expression for the function $\Delta i = i_3 - i_2$, applying the condition $t_1 \gg t_2 \gg t_3$. The corresponding technique will be known as reverse differential pulse voltametry (RDPV) for a SMDE or reverse differential pulse polarography (RDPP) for a DME. The name RDNPV or RDNPP is reserved for those conditions where no time restrictions exist in the pulses used. This nomenclature is that commonly used in double-pulse techniques.[11]

In the records corresponding to the RDP techniques, the appearance of two peaks can be observed for an irreversible simple electronic transfer. One of the peaks appears at more positive potentials than the normal reduction potential, $E°$, while the other appears at more negative potentials than $E°$. The difference between the potentials of these peaks enables an approximate determination of the value of k_s (apparent heterogeneous rate constant), while the sum of these peak potentials is proportional to $E°$. Finally, the half-width of the peak, W (width corresponding to the half-height of the peak), permits an approximate calculation of the values of the transfer coefficients α_c in the peak which appears at more negative potentials than $E°$ and α_a in the peak which appears at more positive potentials than $E°$.

The equations obtained have been checked against experimental examples of the well-known systems $(Fe(C_2O_4)_3^{3-}/Fe(C_2O_4)_3^{4-}$ and Cr^{3+}/Cr^{2+}.

EXPERIMENTAL SECTION

Potential pulses and data acquisition were carried out using a 12-bit ADDA card, PC-LabCard PCL818, interfacing a potentiostat AMEL 553 and a PC-compatible computer. In RDP techniques, we are interested in the measure of one value of i_2 (at time t_2) and one value of i_3 (at time t_3). However, the data acquisition program is designed to acquire 10 values of the current along the second potential step (corresponding to times $0.1t_2$, $0.2t$, ..., t_2) and 10 values of the current along the third potential step (corresponding to times $0.1t_3$, $0.2t_3$, ..., t_3). In this form we can construct with only one experiment 10 RP curves and 10 RDP curves. To diminish the noise present in the digital record of $i-t$ curves, we have made a large oversampling. So, primary data acquisiton was performed at the maximum sampling rate of the device (100 KHz). In each potential step, a second set of 100 experimental data was obtained by averaging primary data; so, if the potential step has a duration of t seconds, each point of the second set was obtained by averaging $1000t$ primary data. Next, we reduce this second 100 point set to the finally desired 10 point set. For this purpose, we divide the duration of the potential step into 10 segments with 10 points each. The points corresponding to each segment were fitted to a second-order polynomial by the least-squares procedure; inserting the value of time desired in the polynomial corresponding to each segment, we obtain the final point. By means of this procedure, we obtain a practically noise-free $i-t$ response. However, occasionally, a pulse-type noise of considerable amplitude was observed. To avoid this interference, each potential sequence was carried out at least twice, and the sequences were compared for a given value of time. If the difference between the two measured values exceeded 1% of the current range in the potentiostat (usually $1-10\ \mu A$), we assumed that some pulse noise is present, and the potential sequences were discarded and repeated. A moving average smoothing procedure[12] was applied on the final $\Delta i-E_2$ curves. This treatment gives rise to a noise-free and apparently undistorted RDP record.

Measurements were made using a thermostated cell, the temperature of which was kept constant at 25 ± 0.1 °C.

A DME was used (Amel, 25 cm) as working electrode. The mercury flow was $m = 1.625$ mg/s for the Fe(III)/Fe(II) system and $m = 0.790$ mg/s for the Cr(III)/Cr(II) system. A saturated calomel electrode and a platinum electrode were used as reference and auxiliary electrodes, respectively.

All reagents were Merck analytical grade and were used without further purification. Mercury was purified with dilute nitric acid and distilled three times in vacuum. Nitrogen gas was used for de-aeration. We compiled with standard safety rules in preparing and handling all solutions and chemical used, particularly Cd^{+2} and Hg. Thus, pipets were filled with the aid of rubber bulbs, amd Hg was purified and distilled in a gas hood and kept under water throughout. Skin contact was avoided by using rubber gloves. Other conditions were as in ref 10.

THEORETICAL BACKGROUND

Consider the following electrode reduction process:

$$A + ne^- \rightleftharpoons B$$

The definition $\Delta i = i_3 - i_2$ can be obtained from eqs 5 and 30 in ref 10 without constraints on either potentials or the interval over which the different potentials are applied. However, in this work we shall impose the following conditions: $t_1 \gg t_2 \gg t_3$. Therefore, for an SMDE and/or a DME,

$$\frac{\Delta i}{i_{dp}} = F(\omega)\left[\frac{\gamma K_2(1-\varrho)}{(1+\gamma K_3)(1+\gamma K_2)} + \frac{2\eta}{Y}\sqrt{\frac{\beta}{\pi}}\left(1 - \frac{2F(Y)}{\sqrt{\pi}Y}\right) - \frac{2F(Y)\eta\gamma K_2}{\sqrt{\pi}Y(1+\gamma K_2)}\right] + \frac{F(Y)\gamma K_2}{(1+\gamma K_2)}\left(\sqrt{\frac{\lambda}{1-\lambda}} - \sqrt{\lambda}\right) \quad (1)$$

where

$$i_{dp} = nFq_0\sqrt{D_A/\pi t_3}C_A^*(t_1+t_2+t_3)^z \quad (2)$$

$$K_i = \exp[nF(E_i - E°)/RT] \qquad \text{for } i = 2, 3 \quad (3)$$

$$\varrho = \exp[nF\Delta E/RT] = K_3/K_2 \quad (4)$$

$$\eta = 1 - \frac{1+\gamma K_2}{1+\gamma K_3}\varrho^\alpha \quad (5)$$

$$\lambda = t_3/(t_2+t_3) \quad (6)$$

$$\beta = \frac{(t_2+t_3)}{(t_1+t_2+t_3)}(2z+1) \quad (7)$$

$$\gamma = \sqrt{D_A/D_B} \quad (8)$$

(11) Osteryoung, J.; Schreiner, M. M. *CRC Crit. Rev. Anal. Chem.* **1988**, *19*, S1.

(12) Savitzky, A.; Golay, M. J. E. *Anal. Chem.* **1964**, *36*, 1627.

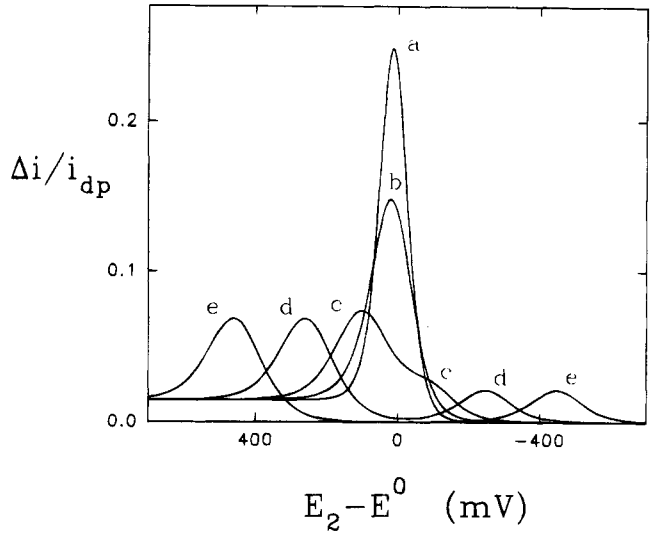

Figure 2. Plot of $\Delta i/i_{dp}$ vs $E_2 - E^\circ$ with $\Delta E = -25$ mV, $z = 0$, $n = 1$, $\alpha = 0.5$, $D_A = D_B = 10^{-5}$ cm²/s, $t_1 = 3$ s, $t_2 = 0.3$ s, $t_3 = 0.03$ s, and k_s = (a) 1, (b) 5×10^{-3}, (c) 10^{-3}, (d) 5×10^{-5}, and (e) 10^{-6} cm/s.

$$Y = \sqrt{\frac{4(t_2 + t_3)}{D_A}}\, k_s \frac{1 + \gamma K_2}{K_2^{\alpha}} \tag{9}$$

$$\omega = \sqrt{\frac{4t_3}{D_A}}\, k_s \frac{1 + \gamma K_3}{K_3^{\alpha}} \tag{10}$$

$$F(x) = \sqrt{\pi}\frac{x}{2}\exp\left(\frac{x^2}{4}\right)\operatorname{erfc}\left(\frac{x}{2}\right) \approx \frac{1}{0.658 + [(1 - 0.658)^2 + (4/\pi x^2)]^{1/2}} \tag{11}$$

Equation 1 has been derived for any plane electrode whose area increases with an arbitrary power of time, $q(t) = q_0 t^z$, where $z = 0$ for a SMDE and $z = {}^2/_3$ for a DME. Moreover, E° is the normal reduction potential, k_s is the apparent heterogeneous rate constant for the charge transfer at E°, α is the transfer coefficient, and D_A and D_B are the diffusion coefficients of species A and B. Finally, the $F(x)$ function is defined in eq 11 in a rigorous form (first equality) as well as in an approximate one (second equality). The use of the approximate expression leads to an error of, at most, 0.4%.[13]

We have compared eq 1 and the general solution given in ref 10, in which no restrictions are assumed on pulse duration. We have found that the error committed by using eq 1 is <5%, provided that $t_2/t_1 \leq 0.2$ and $t_3/(t_1 + t_2) \leq 0.02$.

Figure 2 shows some examples of the application of eq 1 for different values of k_s, with $t_1 = 3$ s, $t_2 = 0.3$ s, $t_3 = 0.03$ s, $\Delta E = -25$ mV, and $z = 0$. The remaining parameters are given in the figure caption. For $k_s \geq 10^{-1}$ cm/s, only one peak appears, and its position and height are independent of the k_s value, i.e., under these experimental conditions and for the RDP technique, the electronic transfer can be considered as totally reversible. In these conditions ($k_s \geq 10^{-1}$ cm/s), eq 1 may be simplified to

$$\frac{\Delta i}{i_{dp}} = \frac{\gamma K_2(1 - \varrho)}{(1 + \gamma K_3)(1 + \gamma K_2)} + \frac{\gamma K_2 \lambda^{3/2}}{2(1 + \gamma K_2)} \tag{12}$$

The first term of the right-hand side in this equation coincides with the response obtained for a reversible process in differential pulse voltametry (DPV) and differential pulse polarography (DPP).[14] For this reason, no exhaustive analysis of this term will be carried out.

The second term of the right-hand side of eq 12 tends to $\lambda^{3/2}/2$ when $E_2 \to \infty$ ($K_2 \to \infty$). This term is responsible for the current plateau observed in the records for very positive values of E_2 (see Figure 2). The value of Δi in this plateau (Δi_m) is given by $\Delta i_m = 0.5 i_{dp}\lambda^{3/2}$. Therefore, the measurement of Δi_m enables us to obtain an approximate value of i_{dp}.

For $k_s < 5 \times 10^{-4}$ cm/s, eq 1 can be simplified to

$$\frac{\Delta i}{i_{dp}} = \frac{2\eta F(\omega)}{\sqrt{\pi Y}}\left(\sqrt{\beta}\left(1 - \frac{2F(Y)}{\sqrt{\pi Y}}\right) - \frac{F(Y)\gamma K_2}{1 + \gamma K_2}\right) + \frac{F(Y)\gamma K_2 \lambda^{3/2}}{2(1 + \gamma K_2)} \tag{13}$$

Under these conditions, two well-developed peaks can be observed in the $\Delta i - E_2$ curves (see Figure 2). This peculiar behavior is characteristic of this technique, and it is not observed in DPV or DPP techniques.

To obtain eq 12 and 13 from eq 1, we have taken into account that the term $[\lambda(1 - \lambda)]^{1/2} - \lambda^{1/2}$ can be taken approximately as $\lambda^{3/2}/2$, since $\lambda \ll 1$ when $t_1 \gg t_2 \gg t_3$.

From eq 13, corresponding to an irreversible process, we can obtain individual expressions for each peak. So, when $E_2 \ll E^\circ$ (reduction peak), eq 13 becomes

$$\left[\frac{\Delta i}{i_{dp}}\right]^{red} = \frac{2(1 - \varrho_c)F(\omega)}{Y}\sqrt{\frac{\beta}{\pi}}\left(1 - \frac{2F(Y)}{\sqrt{\pi Y}}\right) \qquad \text{for } E_2 \ll E^\circ \tag{14}$$

This peak appears at practically the same potential as the reduction peak in the DPV or DPP techniques.

It is useful redefine in eq 14 $\alpha_c = \alpha n$. Therefore, we can write

$$Y = \sqrt{4(t_2 + t_3)/D_A}\, k_s\, e^{[-\alpha_c F(E_2 - E^\circ)]/RT} \qquad \text{for } E_2 \ll E^\circ \tag{15}$$

$$\omega = \sqrt{4t_3/D_A}\, k_s\, e^{[-\alpha_c F(E_3 - E^\circ)]/RT} \qquad \text{for } E_3 \ll E^\circ \tag{16}$$

and

$$\varrho_c = e^{\alpha_c F \Delta E/RT} \tag{17}$$

On the other hand, when $E_2 \gg E^\circ$, the reoxidation of species B takes place, and eq 13 leads to the following expression for the reoxidation peak:

$$\left[\frac{\Delta i}{i_{dp}}\right]^{reox} = \frac{2(1 - \varrho_a)F(\omega)}{\sqrt{\pi Y}}\left[\sqrt{\beta}\left(1 - \frac{2F(Y)}{\sqrt{\pi Y}}\right) - F(Y)\right] + \frac{F(Y)\lambda^{3/2}}{2} \qquad \text{for } E_2 \gg E^\circ \tag{18}$$

where in this equation, $\alpha_a = (1 - \alpha)n$ and

$$Y = \sqrt{4(t_2 + t_3)/D_A}\, k_s\, e^{[\alpha_a F(E_2 - E^\circ)]/RT} \qquad \text{for } E_2 \gg E^\circ \tag{19}$$

$$\omega = \sqrt{4t_3/D_A}\, k_s\, e^{[\alpha_a F(E_3 - E^\circ)]/RT} \qquad \text{for } E_3 \gg E \tag{20}$$

and

(13) Sánchez-Maestre, M.; Muñoz, E.; Avila, J. L.; Camacho, L. *Electrochim. Acta* **1992**, *37*, 1129.

(14) Parry, E. P.; Osteryoung, R. A. *Anal. Chem.* **1965**, *37*, 1634.

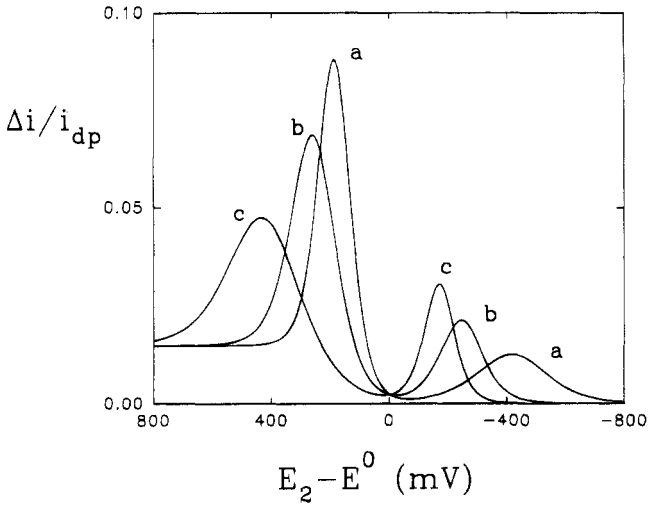

Figure 3. Plot of $\Delta i/i_{dp}$ vs $E_2 - E^\circ$ with $\Delta E = -25$ mV, $z = 0$, $\alpha_c + \alpha_a = 1$, $D_A = D_B = 10^{-5}$ cm²/s, $t_1 = 3$ s, $t_2 = 0.3$ s, $t_3 = 0.03$ s, $k_s = 5 \times 10^{-5}$ cm/s and α_c = (a) 0.3, (b) 0.5, and (c) 0.7.

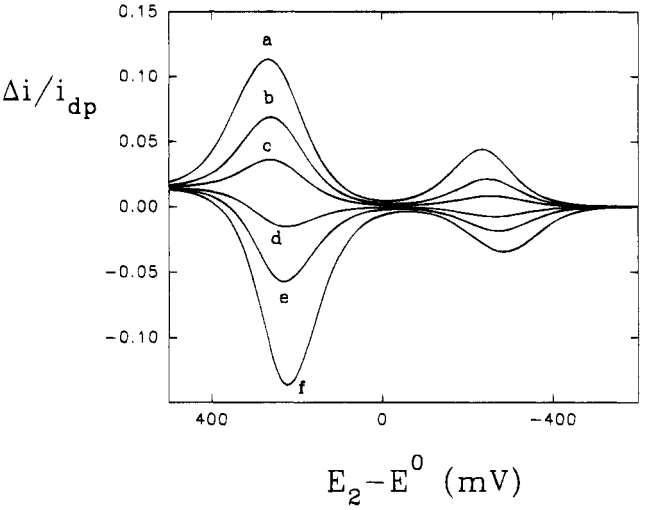

Figure 4. Plot of $\Delta i/i_{dp}$ vs $E_2 - E^\circ$ with $z = 0$, $\alpha_c = \alpha_a = 0.5$, $D_A = D_B = 10^{-5}$ cm²/s, $t_1 = 3$ s, $t_2 = 0.3$ s, $t_3 = 0.03$ s, $k_s = 5 \times 10^{-5}$ cm/s, and ΔE = (a) −50, (b) −25, (c) −10, (d) 10, (e) 25, and (f) 50 mV.

$$\varrho_a = e^{-\alpha_a F \Delta E/RT} \tag{21}$$

In eq 14 and 18, the superscripts red and reox indicate the peaks which appear at more negative and more positive potentials than E°, respectively.

It can be noticed that, in Figure 2, Δi is positive for both reduction and reoxidation processes, due to the fact that $\Delta E = E_3 - E_2 < 0$. Conversely, for $\Delta E > 0$, Δi is always negative.

Figure 3 shows the influence of the transfer coefficients, α_c and α_a, predicted by eqs 13 or 14 and 18, on the Δi–E_2 curves for $k_s = 5 \times 10^{-5}$ cm/s, $\alpha_c + \alpha_a = 1$, and the remaining conditions as in Figure 2. As can be seen, when α_c decreases, the reduction peak decreases in height and widens, while the reoxidation peak becomes higher and narrower.

By defining the peak half-width, W, as the width in mV corresponding to the half-height of the peak, when ΔE is small, the half-width is $W_{red} \simeq 92/\alpha_c$ for the reduction peak and $W_{reox} \simeq 92/\alpha_a$ for the reoxidation peak. These two relations, which are only approximate, may be used for an initial estimation of α_c and α_a values, and subsequently these values can be used as input data in a more exact numerical adjustment of experiments.

We have also used eqs 13 or 14 and 18 to obtain the influence of ΔE on the Δi–E_2 curves. This influence is shown in Figure 4, for $k_s = 5 \times 10^{-5}$ cm/s and the remaining parameters as in Figure 3. For this figure, we have used both negative and positive ΔE values. It can be seen that as the absolute value of ΔE increases, the reoxidation peaks, both for $\Delta i > 0$ ($\Delta E < 0$) and for $\Delta i < 0$ ($\Delta E > 0$), become relatively higher than the corresponding reduction peaks.

For a small absolute ΔE value, the potentials of the peaks observed can be expressed approximately by

$$E_p^{red} \approx E^\circ - \Delta E/2 + RT/\alpha_c F \ln(k_s\sqrt{\pi t_3/D_A\sqrt{\lambda}}) \tag{22}$$

$$E_p^{reox} \approx E^\circ - \Delta E/2 - RT/\alpha_a F \ln(\gamma k_s\sqrt{\pi t_3/D_A\sqrt{\lambda}}) \tag{23}$$

The approximate values of E° and k_s can be obtained by combining eqs 22 and 23:

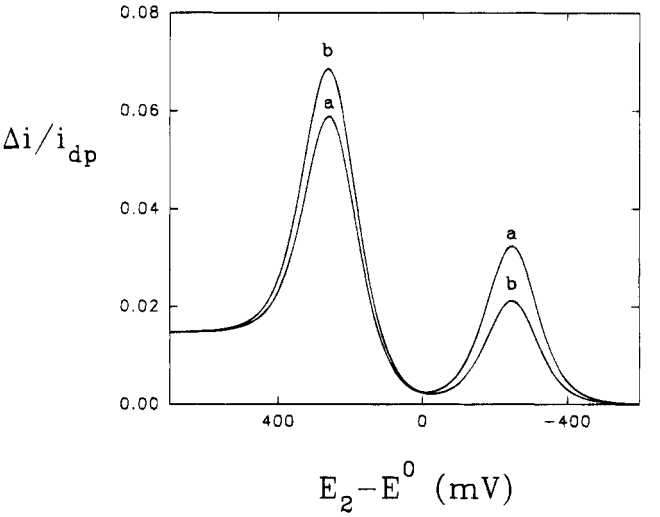

Figure 5. Plot of $\Delta i/i_{dp}$ vs $E_2 - E^\circ$ with $\Delta E = -25$ mV, $\alpha_c = \alpha_a = 0.5$, $D_A = D_B = 10^{-5}$ cm²/s, $t_1 = 3$ s, $t_2 = 0.3$ s, $t_3 = 0.03$ s, $k_s = 5 \times 10^{-5}$ cm/s, and z = (a) 0 and (b) $^2/_3$.

$$k_s \approx \gamma^{[\alpha_c+\alpha_a]/\alpha_c}\sqrt{D_A\sqrt{\lambda}/\pi t_3}\,\exp\left[\frac{\alpha_c\alpha_a F}{(\alpha_c+\alpha_a)RT}(E_p^{red} - E_p^{reox})\right] \tag{24}$$

$$E^\circ \approx [E_p^{red} + E_p^{reox} + \Delta E]/2 + \frac{RT}{(\alpha_c+\alpha_a)F}\ln(\gamma) - \frac{(\alpha_a-\alpha_c)}{2(\alpha_c+\alpha_a)}(E_p^{red} - E_p^{reox}) \tag{25}$$

Figure 5 shows an example of the influence of the value of z on the Δi–E_2 curves ($z = 0$ for a SMDE and $z = ^2/_3$ for a DME) for an irreversible process. When we compare the results obtained for $z = 0$ and $z = ^2/_3$, the ratio between the heights of the reoxidation peak and the reduction peak ($\Delta i_p^{reox}/\Delta i_p^{red}$) is greater for a DME than for a SMDE. The remaining parameters, such as the half-width of the peaks or the peak potentials, are scarcely affected by the value of z.

DISCUSSION AND EXPERIMENTAL APPLICATIONS

An experimental study of curves Δi vs E_2 has been carried out for two different experimental systems. We have analyzed

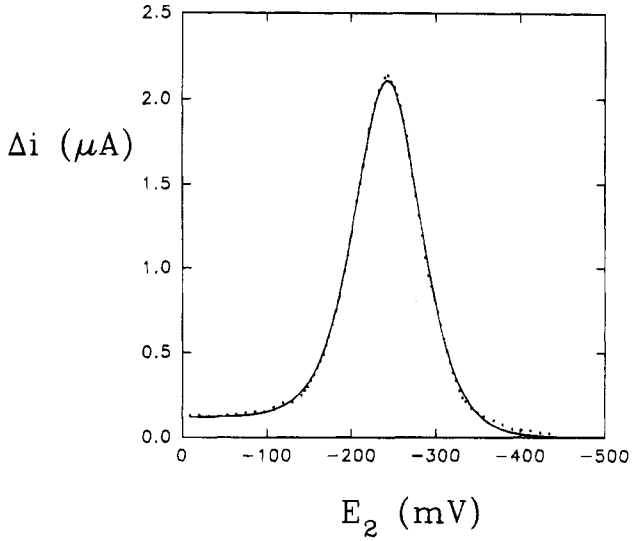

Figure 6. RDP plot of Δi vs E_2 for 5×10^{-4} M Fe(III) in $K_2C_2O_4$, 0.45 M (points), at $\Delta E = -25$ mV, $t_1 = 3$ s, $t_2 = 0.3$ s, $t_3 = 0.03$ s, and $z = {}^2/_3$ (DME). The full curve corresponds to the predictions of eq 1 for $E_{1/2} = E^\circ + (RT/2nF) \ln(D_B/D_A) = -256$ mV, $D_A = 4.3 \times 10^{-6}$ cm^2/s, and $n = 1$.

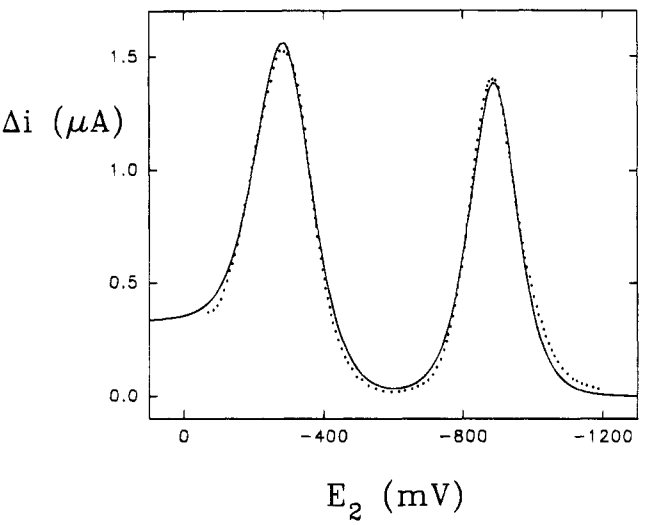

Figure 7. RDP plot of Δi vs E for 2×10^{-3} M Cr(III) in $NaClO_4$, 0.5 M (points), at $\Delta E = -50$ mV, $t_1 = 3$ s, $t_2 = 0.4$ s, $t_3 = 50$ ms, and $z = {}^2/_3$ (DME). The full curve corresponds to the predictions of eqs 14 and 18 for $\alpha_c = 0.52$, $\alpha_a = 0.47$, $E^\circ = -612$ mV, $k_s = 1.1 \times 10^{-5}$ cm/s, and $D_A = D_B = 5.4 \times 10^{-6}$ cm^2/s.

both a reversible electrode process ($Fe(C_2O_4)_3^{3-}$) and a totally irreversible one (Cr^{3+}).

Figure 6 shows the experimental $\Delta i - E_2$ record (points) carried out for a solution of Fe^{3+} at a concentration of 5×10^{-4} M in $C_2O_4^{2-}$, 0.45 M. This experiment was performed on a DME with $\Delta E = -25$ mV, $t_1 = 3$ s, $t_2 = 0.3$ s, and $t_3 = 30$ ms. It has previously been determined that for the pair $Fe(C_2O_4)_3^{3-}/Fe(C_2O_4)_3^{4-}$, $k_s = 1.44$ cm/s.[15] This value of k_s assures that the electrode process is totally reversible under the experimental conditions employed here.

The experimental values shown in Figure 6 have been numerically adjusted to eq 12, using the program SigmaPlot.[16]

$E_{1/2} = E^\circ + (RT/2nF) \ln(D_B/D_A)$ and D_A have been used as unknown parameters in the numerical adjustment. In this case, D_A is the diffusion coefficient for $Fe(C_2O_4)_3^{3-}$, and D_B is the diffusion coefficient for ($Fe(C_2O_4)_3^{4-}$). The values obtained in the numerical adjustment are $E_{1/2} = -256 \pm 1$ mV and $D_A = (4.3 \pm 0.2) \times 10^{-6}$ cm^2/s. The values in the literature for D_A are, in general, close to the value reported in this paper ($D_A = 4.8 \times 10^{-6}$ cm^2/s.[15,17,18]

The value of D_B cannot be obtained from our experimental results, since E° and D_B are not independent parameters in eq 12. However, D_B can be obtained from the current i_2 (RP), used in the calculation of $\Delta i = i_3 - i_2$. However, the ferrioxalate system did not require calculation of D_B since, as shown in the literature, $D_A = D_B$.[17,18] Figure 6 shows that the agreement between the experimental data and the theoretical predictions (eq 12) for the above values of $E_{1/2}$ and D_A is excellent.

Figure 7 shows the experimental $\Delta i - E_2$ curves (points) carried out for a solution of 2×10^{-3} M Cr(III) in $NaClO_4$, 0.5 M. As in the previous case, this experiment was performed on a DME, with $\Delta E = -50$ mV, $t_1 = 3$ s, $t_2 = 0.4$ s, and $t_3 = 50$ ms. As can be seen in the record, two current peaks appear, corresponding to an irreversible process (eq 13 or eq 14 and 18).

The numerical adjustment of experimental data to eqs 14 and 18 requires knowledge of the following six parameters: α_c, α_a, k_s, E°, D_A, and D_B. As is suggested,[19] we can assume $D_A \approx D_B$. In opposition to the reversible case, D_B can be obtained in the numerical adjustment. However, it is convenient to reduce the number of adjustable parameters in order to remove interdependence problems from the determined parameters.

By following the procedure described in the previous section, we can obtain an estimation of the values of α_c ($\alpha_c \approx 92/W_{red}$), α_a ($\alpha_a \approx 92/W_{reox}$), D_A (from i_{dp}, see eq 2 and $i_{dp} \approx 2\Delta i_M \lambda^{-3/2}$), E° (eq 25), and k_s (eq 24). From Figure 7, we deduce $W_{red} = 165$ mV, $W_{reox} = 212$ mV, $\Delta i_m = 0.3$ μA, $E_p^{red} = -286$ mV, and $E_p^{reox} = -880$ mV; therefore, taking $\gamma = 1$, $\alpha_c \simeq 0.56$, $\alpha_a \simeq 0.43$, $D_A \approx 5 \times 10^{-6}$ cm^2/s, $E^\circ \simeq -608$ mV, and $k_s \simeq 1.2 \times 10^{-5}$ cm/s. These values have been used as starting points for the numerical adjustment of experimental data to eq 14 and 18, by means of SigmaPlot.[16] The values obtained are $\alpha_c = 0.52 \pm 0.02$, $\alpha_a = 0.47 \pm 0.02$, $E^\circ = -612 \pm 2$ mV, $k_s = (1.1 \pm 0.1) \times 10^{-5}$ cm/s, and $D_A = (5.4 \pm 0.4) \times 10^{-6}$ cm^2/s. The solid line in Figure 7 shows the predicted Δi vs E_2 curve (eqs 14 and 18) with these parameters.

The obtained parameters can be compared with those given in the literature. Zielinska-Ignaciuk and Galus[19] found $\alpha_c = 0.55$ and $\alpha_a = 0.46$ in $NaClO_4$, independent of the concentration of $NaClO_4$. On the other hand, Andreu et al.[20] have reported $D_A = 5.9 \times 10^{-6}$ cm^2/s and $E^\circ = -650$ mV (vs SCE) in 0.5 M $NaClO_4$. Moreover, k_s can be obtained from the data in Figure 1 in ref 20. The value that we obtain from this figure is $k_s = 1.4 \times 10^{-5}$ cm/s. As can be observed, the kinetic parameters given in the literature are in good accordance with those obtained in this paper. The value of E° is, however, in some disagreement, but this value is strongly dependent on the concentration of supporting electrolyte.[19]

As is stated above, the mathematical model used in this work takes no account of electrode sphericity, which can generate some errors in the determination of the parameters, mainly D_A. The

(15) Rohko, T.; Kogoma, M.; Aoyagui, S. *J. Electroanal. Chem.* **1972**, *38*, 45.
(16) *SigmaPlot;* Jandel Scientific, 65 Koch Rd., Corte Madera, CA 94925.
(17) Struijs, J.; Sluyters-Rehbach, M.; Sluyters, J. H. *J. Electroanal. Chem.* **1983**, *146*, 263.
(18) Myland, J.; Oldham, K. B.; Zoski, C. *J. Electroanal. Chem.* **1985**, *193*, 3.
(19) Zielinska-Ignaciuk, M.; Galus, *Z. J. Electroanal. Chem.* **1974**, *50*, 41.
(20) Andreu, R.; Rueda, M.; González-Arjona, D.; Sánchez, F. *J. Electroanal. Chem.* **1984**, *175*, 251.

quantitative estimation of this error cannot be carried out, since the general solution for the third potential pulse with spherical diffusion does not exist in the literature. However, under certain conditions, the error can be estimated. The subject is discussed below.

Let us consider an SMDE for the sake of simplicity. In the RDP technique, $E_1 \rightarrow -\infty$ ($K_1 = 0$), where, independent of whether amalgamation takes place or not, the current of this first pulse is given by

$$i_1(t_1) = nFAC^* \sqrt{D_A/\pi t_1}\,(1 + \sqrt{\pi D_A t_1}/r_0) \qquad (26)$$

However, i_1 is not used directly in the function of the current, which is defined in RDP techniques as $(i_3 - i_2)$.

The general solution for i_2 for a reversible process taking into account the electrode sphericity exists in the literature.[7,21,22] If, for the sake of simplicity, we choose diffusion conditions in this second pulse ($E_2 \rightarrow \infty$, $K_2 = \infty$), we can write[22]

$$i_2(t_1 + t_2) = i_1(t_1 + t_2) - nFAC^* \sqrt{D_A/\pi t_2}\left[1 + \sqrt{\pi D_A t_2}/r_0\left(\frac{(\gamma \mp 1)2g_0(\beta)}{\gamma\pi\sqrt{\beta}} \pm \frac{1}{\gamma}\right)\right] \qquad (27)$$

with $\gamma = (D_A/D_B)^{1/2}$, $\beta = t_2/(t_1 + t_2)$, and

$$g_0(\beta) = \sqrt{\beta}\,\arcsin(\sqrt{\beta}) + \sqrt{1 - \beta} \qquad (28)$$

Where two signs appear in eq 27, the upper one refers to the soluble product and the lower one to the formation of an amalgam.

The error in the calculation of i_2 where spherical correction is not taken into account if the amalgamation takes place or if $D_A \neq D_B$ has two origins. The first proceeds from $i_1(t_1 + t_2)$. The second is determined by the second term in brackets in eq 27, which can reach values higher than unity. However, in the case of a soluble product and $\gamma = 1$, eq 27 reduces to

$$i_2(t_1 + t_2) = i_1(t_1 + t_2) - nFAC^* \sqrt{D_A/\pi t_2}(1 + \sqrt{\pi D_A t_2}/r_0) \qquad (29)$$

In the literature there does not exist a general solution to the third potential pulse with spherical correction when the product is amalgamated or $D_A \neq D_B$. Recently, however, we have obtained the solution for a third potential pulse for a reversible process on a spherical electrode, with $D_A = D_B$, and for a product soluble in the electrolytic solution.[23] This solution for a SMDE is given by

$$i_3(t_1 + t_2 + t_3) = i_2(t_1 + t_2 + t_3) - nFAC^* \sqrt{D_A/\pi t_3}\left(\frac{K_2(1 - \varrho)}{(1 + K_3)(1 + K_2)}\right)(1 + \sqrt{\pi D_A t_3}/r_0) \qquad (30)$$

Then, under conditions where eq 30 holds, the error in i_3 through not considering the electrode sphericity has three contributions. The first one is due to the term $\{1 + (\pi D_A t_3)^{1/2}/r_0\}$, which for the Fe(III)/Fe(II) system ($t_3 = 0.03$ s, $r_0 = 0.045$ cm, and $D_A = 4.3 \times 10^{-6}$ cm^2/s) is 1.014. The other two sources of error are the same that those indicated for i_2.

Equation 30 can be used to estimate the magnitude of error made when eq 12 of this paper, which neglects electrode sphericity, is used. Indeed, from eq 30, it is immediately deduced that, if the condition $t_3 \ll t_1 + t_2$ is fulfilled, which implies that $i_2(t_1 + t_2) \approx i_2(t_1 + t_2 + t_3)$, then, taking into account eq 2, eq 30 changes to

$$\frac{\Delta i}{i_{dp}} = \frac{i_3(t_1 + t_2 + t_3) - i_2(t_1 + t_2)}{i_{dp}} \approx \frac{K_2(1 - \varrho)}{(1 + K_3)(1 + K_2)}(1 + \sqrt{\pi D_A t_3}/r_0) \qquad (31)$$

Equation 31 shows that when $t_3 \ll t_1 + t_2$, $D_A = D_B$ and, for a reversible process, Δi increases by a factor $\{1 + (\pi D_A t_3)^{1/2}/r_0\}$ relative to the solution obtained for a planar electrode. It is clear that, in the particular case of the Fe(III)/Fe(II) system, the error resulting from not considering sphericity is ~1.4%, which is within the normal measurement error range. In any case, the error is quite significant in the presence of amalgamation. When $D_A \neq D_B$ and the product is soluble, the magnitude of the error made in the third pulse cannot be strictly assessed from eq 31; however, it must be much smaller than that made in the presence of amalgamation. Nevertheless, the error for the second pulse can be estimated from eq 27.

The records in Figures 6 and 7 show the enormous potentially of the RDP technique from the kinetic point of view. Indeed, this technique allows an analysis of irreversible processes in quite a simple way and permits us to obtain the same information as cyclic voltametry, even though, in our case, we work with easily programmable analytical functions for the realization of numerical adjustments. Moreover, this technique possesses the advantages inherent to DP techniques, such as the partial elimination of the charging current and the increases in the sensitivity and detection limit. The sensitivity to the elucidation of kinetic parameters is at least as good as that of other electrochemical techniques, such as cyclic voltammetry.

ACKNOWLEDGMENT

The authors wish to express their gratitude to the Junta de Andalucia, to the DREUCA de la Region de Murcia (Project PB91/025), and to the DGICyT (Projects PB91-0834 and PB90-0307) for financial help granted. We would also like to express our gratitude to the reviewers, who have greatly helped us improve the paper.

Received for review July 7, 1994. Accepted May 14, 1995.[⊗]

AC940681E

(21) Goodisman, J. *J. Electroanal. Chem.* **1983**, *144*, 33.
(22) Molina, A.; Serna, C.; Chicón, R.; Camacho, L.; Ruiz, J. J. *Can. J. Chem.* **1994**, *72*, 2378.
(23) Molina, A.; Serna, C.; Camacho, L. *J. Electroanal. Chem.* In press.

[⊗] Abstract published in *Advance ACS Abstracts*, June 15, 1995.